# EXTREME WAVE GENERATION, BREAKING AND IMPACT SIMULATIONS WITH REEF3D

Hans Bihs*, Arun Kamath and Mayilvahanan Alagan Chella and Øivind A. Arntsen

Department of Civil and Environmental Engineering, Norwegian University of Science and Technology (NTNU), 7491 Trondheim, Norway

*36th International Conference on Ocean, Offshore and Arctic Engineering, OMAE2017 Trondheim*, 2017, - -, pp. -.
DOI: http://dx.doi.org/10.1115/OMAE2017-61524

## ABSTRACT

An accurate description of extreme waves is necessary in order to estimate maximum wave forces on offshore structures. On several occasions freak waves have been observed in the past, some causing severe damage. In order to model such extreme wave conditions with a computational fluid dynamics (CFD) model, emphasize needs to be put on the wave generation. One possibility is to use focused waves of first or second order based on irregular sea state wave spectra. For focused waves, the wave phase is chosen, so that the waves focus in a predetermined location at a specified time. Numerical tests have shown, that generating extreme waves based on this method is somewhat limited. The individual wave components are steep enough, that they start to break before the focus location. In the current paper, transient wave packets are used for extreme wave generation. This way, extreme waves can be generated that are higher, but only break at the concentration point. The transient wave packets method is implemented in the open-source CFD software REEF3D. This model uses the level set method for interface capturing. For the hydrodynamics, the Navier-Stokes equations are solved in three dimensions. The code employs a staggered Cartesian mesh, ensuring tight pressure-velocity coupling. Complex geometries are handled with a ghost cell immersed boundary method. High-performance computing is enabled through domain decomposition based parallelization. Convection discretization of the different flow variables is performed with the fifth-order WENO (weighted essentially non-oscillatory) scheme. For the explicit time treatment a third-order Runge-Kutta scheme is selected. In order to validate the extreme wave generation, numerical tests in an empty wave tank are performed and compared with experimental data. Then, the extreme wave breaking on a vertical circular cylinder is investigated.

*Corresponding author, hans.bihs@ntnu.no

# INTRODUCTION

The generation of extreme waves in experimental or numerical wave tanks is a challenging task. At sea, the occurrence of extreme waves is of stochastic nature. Replicating them in a numerical model based on this principle would take prohibitively long time. The best route for extreme wave generation is deterministic. Several numerical studies using focused waves are available in literature (Chen et al., 2014; Paulsen et al., 2014; Bihs et al., 2016*a*). The basis of focused wave generation is irregular wave generation. In the mentioned papers, the JONSWAP wave spectrum is used to determine the wave amplitudes and frequencies of the individual wave components. In contrast to irregular wave generation, where random values are used for the wave phases, the phases for focused waves are manipulated in such a way that all waves focus at a given location and time. As focused waves typically follow the JONSWAP spectrum, the wave components around the spectrum peak are of already large amplitude relatively to the focused wave height. The individual harmonic components become relatively steep for increasing focused heights, which introduces two challenges for extreme wave generation based on focused waves: The high steepness of the components introduces non-linearity, which makes the correct prediction of the focusing point and time difficult (Bihs et al., 2016*a*). Also, for larger focusing heights, the wave components start to break prematurely before they reach the focus location.

Another method for extreme wave generation are wave packets. The earlier version of the wave packet method used a symmetric Gaussian spectrum (Clauss and Bergmann, 1986). The Gaussian wave packets have been used for example to generate extreme breaking wave impact on a vertical cylinder in an experimental wave flume (Wienke and Oumeraci, 2005). The wave packets have later been optimised by replacing the Gaussian spectrum with a tailor made one, where the high frequency components have been adjusted for avoiding premature breaking (Clauss and Kuehnlein, 1997). Compared to the focused waves, the spectrum for the wave packets is wider and consists of more harmonic components where each of them is of relatively lower amplitude compared to the focusing height. As a result, larger focusing heights can be achieved, while the components are less affected by nonlinearity and premature breaking.

The wave packets algorithm is implemented in the open-source CFD code REEF3D (Bihs et al., 2016*b*). The model has been used and validated for a wide range of marine applications, such as breaking wave kinematics (Alagan Chella et al., 2016), breaking wave forces (Alagan Chella et al., 2017), floating body dynamics (Bihs and Kamath, 2016), sloshing (Grotle et al., 2016) or sediment transport (Afzal et al., 2015). The wave packets are first validated using experimental data for a non-breaking focused wave. This is extended to a 2D breaking focused wave, which is used for validation and for determination of the breaking point. This information is then used for a 3D case, where the breaking focused wave interacts with a vertical cylinder.

# NUMERICAL MODEL

The incompressible Unsteady Reynolds-Averaged Navier-Stokes (URANS) equations are used to solve the fluid flow problem:

$$\frac{\partial u_i}{\partial x_i} = 0 \tag{1}$$

$$\frac{\partial u_i}{\partial t} + u_j \frac{\partial u_i}{\partial x_j} = -\frac{1}{\rho}\frac{\partial p}{\partial x_i} + \frac{\partial}{\partial x_j}\left[(\nu + \nu_t)\left(\frac{\partial u_i}{\partial x_j} + \frac{\partial u_j}{\partial x_i}\right)\right] + g_i \tag{2}$$

where $u$ is the time averaged velocity, $\rho$ is the density of water, $p$ is the pressure, $\nu$ is the kinematic viscosity, $\nu_t$ is the eddy viscosity, $t$ is time and $g$ is the acceleration due to gravity. Chorin's projection method Chorin (1968) is used for the pressure treatment and a multi-grid PFMG preconditioned BiCGStab solver is used to solve for the pressure using the high-performance solver library HYPRE Center for Applied Scientific Computing (2015)Ashby and Flagout (1996).

Turbulence modelling is carried out through k-$\omega$ model Wilcox (1994) based URANS. The eddy viscosity, $\nu_t$, is bounded to avoid unphysical overproduction of turbulence in strained flow as shown by DurbinDurbin (2009). Free surface turbulence damping is introduced around the interface based on the studies by Naot and Rodi Naot and Rodi (1982) to account for the overproduction of turbulence at the free surface due to the large density gradient.

The fifth-order conservative finite difference Weighted Essentially Non-Oscillatory (WENO) scheme proposed by Jiang et al. Jiang and Shu (1996) is used for the discretization of convective terms for the velocity $u_i$, the level set function $\phi$, turbulent kinetic energy $k$ and the specific turbulent dissipation rate $\omega$. A TVD third-order Runge-Kutta explicit time scheme developed by Harten Harten (1983) is employed for time discretization in the model. This scheme is used for the time advancement of the level set function and the reinitialisation equation.

A Cartesian grid is used in the numerical model for spatial discretization. A ghost cell immersed boundary method (IBM) Berthelsen and Faltinsen (2008) is used to incorporate the boundary conditions for complex geometries.The free surface is obtained using the level set method where the zero level set of a signed distance function, $\phi(\vec{x}, t)$ is used to represent the interface between air and water. The level set function is reinitialised after every iteration using a partial differential equation (PDE) based reinitialisation procedure presented by Sussman et al.Sussman et al. (1994) to retain its signed distance property after convection. The computational efficiency of the program is increased by using MPI (Message Passing Interface) to run it as a fully parallel code on multiple processors.

## Wave Packets Generation

The wave packets generation uses a shape amplitude Fourier spectrum of the form Henning (2005):

$$|F| = \frac{27\left(\omega - \omega_{beg}\right)\left(\omega - \omega_{end}\right)^2}{4\left(\omega_{end} - \omega_{beg}\right)^3} \tag{3}$$

Here, $\omega$ is the angular frequency and the subscripts *beg* and *end* confine the Fourier spectrum on the x-axis. The absolute magnitude of the resulting wave amplitude $A_i'$ does not represent the given focused wave input at this point, so a scaling factor $f$ is calculated:

$$f = \frac{A_{focus}}{\sum_{i=1}^{N} A_i'} \tag{4}$$

Then the amplitudes of the harmonic components can be calculated as:

$$A_i = f A_i' \tag{5}$$

The free surface, $\eta^{(1)}$ at the wave generation is then calculated as:

$$\eta^{(1)} = \sum_{i=1}^{N} A_i cos\theta_i \tag{6}$$

where, $A_i$ is the amplitude of the each wave component and $\theta_i$ is the phase of the each component, which is defined as:

$$\theta_i = k_i x - \omega_i t - \epsilon_i \tag{7}$$

where $k_i$ is the wave number of each component. The parameter $\epsilon_i$ is the phase angle, which is chosen in such a way that each wave component focuses at a specified time $t_F$ and location $x_F$.

Second-order irregular wave theory is used as it takes into account wave-wave interaction. The second-order part is added to first-order part for the free surface and the flow velocities:

$$\eta = \eta^{(1)} + \eta^{(2)} \tag{8}$$

$$u = u^{(1)} + u^{(2)} \tag{9}$$

$$w = w^{(1)} + w^{(2)} \tag{10}$$

The second-order wave components are implemented using second-order irregular wave theory Schäffer (1996) as formulated by Ning et al. Ning et al. (2009). At the inlet, the free surface and velocities are prescribed through a simple Dirichlet boundary condition. At the downstream end of the tank, waves are absorbed using active wave absorption.

# RESULTS

## Validation of wave generation in the numerical wave tank

Experimental wave packet data measured in the Large Wave Flume (GWK), Hannover, Germany Pakozdi (2005) is reproduced in the numerical wave tank to validate the CFD model. The experiments were carried out in a 300 m long channel with a water depth of $d = 4.01$ m. The wave packets were generated using a Piston-type wavemaker such that the wave focus at a distance of $x_f = 126.21$ m from the wavemaker at time $t_f = 103$ s with a focussing amplitude of $A_f = 0.75$ m. In order to replicate these results, a 2D numerical wave tank 150 m long with a water depth of $d = 4.01$ m is used with a grid size of $dx = 0.05$ m. The distance of the focus point and the time of focussing is the same as in the experiments with $x_f = 126.21$ m and $t_f = 103$ s. The free surface elevations are measured at several locations in the numerical wave tank are compared to experimental observations and presented in Figs.(1a-1e).
The generated waves seen in Fig. (1a) consist of individual waves of different wave heights and frequencies. Figure 1b shows the propagation of the waves while mostly retaining their form at $x_2 = 50.05$ m. The waves begin to converge as they propagate further to $x_3 = 79.05$ m and $x_4 = 100.10$ m, as seen in Figs. (1c) and (1d). The wave packet focuses at the prescribed

location $x_f = 126.21$ at the prescribed time $x_t = 103.0$ s as seen in Fig. (1e). The numerical results from REEF3D agree well with the experimental data for the wave packet generation, propagation and focussing process throughout the length of the domain.
The free surface in the numerical wave tank at $t = 76.0$ s and $t_f = 103.0$ s are presented in Figs. (2a) and (2b) respectively.

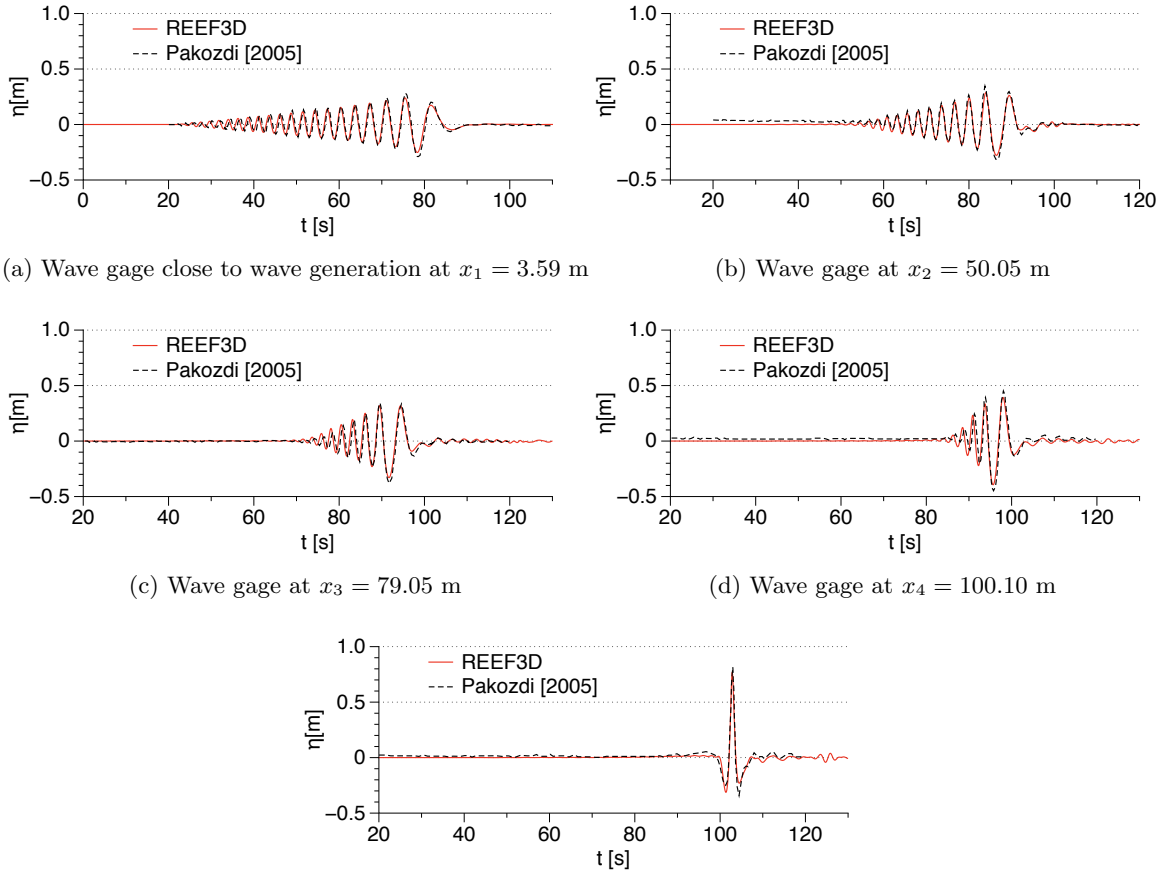


(a) Wave gage close to wave generation at $x_1 = 3.59$ m

(b) Wave gage at $x_2 = 50.05$ m

(c) Wave gage at $x_3 = 79.05$ m

(d) Wave gage at $x_4 = 100.10$ m

(e) Wave gage at the focus point at $x_f = 126.21$ m

Figure 1: Comparison of the numerical results and experimental data for propagation of wave packets focussing at $x_f = 126.21$ m and $t = 103.0$ s

## Replication of wave packet focusing in a shorter numerical domain

The validation of the numerical wave tank for the generation, propagation and focusing of the wave packets is carried out such that the length of the numerical wave tank spans over the distance the wave packets propagated in the experiments before focusing. In order to reduce the computational demand of simulations with focused wave packets, it is prudent to replicate the results in a numerical wave tank of a shorter length. In this section, the length of the numerical wave tank is gradually reduced from 150 m to 25 m to reproduce the same wave as in the previous section. A grid size of $dx = 0.05$ m is used in all the cases.

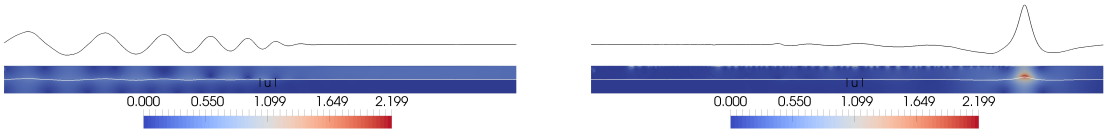


(a) Free surface elevation showing wave packets in the tank at $t = 76.0$ s

(b) Free surface elevation showing the focussed wave at $t = 103.0$ s

Figure 2: Free surface elevation in the numerical wave tank with velocity magnitude contours and magnified free surface showing the propagation and focussing of the wave packets

A simulation is carried out for focussing of the wave packets in a 100 m long tank with a focus distance of $x_f = 90.0$ m at time $t_f = 60.0$ s. The focusing amplitude $A_f$ =0.75 m, the same as that in the validation case presented in the previous section in a 150 m long wave tank. The free surface elevation calculated at the focus point in the 100 m tank is compared to the numerical result from the 150 m and presented in Fig. (3). The free surface elevation from the 150 m long tank is shifted to compare the results in the two cases. The figure shows that the focus height of the wave is correctly reproduced when the focus distance is reduced from 126.21 m to 90.0 m.

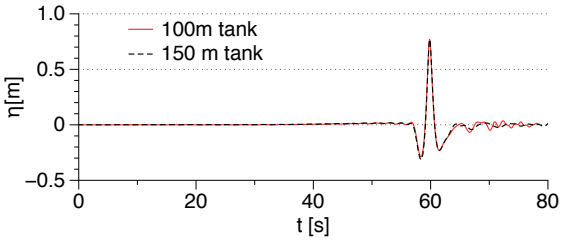


Figure 3: Wave gage at the focus point at $x_f = 90.0$ m for the 100 m tank compared to results from the 150 m tank with $x_f = 126.21$ m

A similar comparison is carried out by repeating the simulation in a 50 m long wave tank with a focus distance of $x_f = 35$ m and focus time $t_f = 25.0$ s. The numerical result for the free surface elevation at the focus point in this case is compared with the focused wave obtained in the 150 m long tank and presented in Fig.(4). It is seen in the figure that the focused wave height is again correctly represented in the smaller wave tank with a reduced distance of propagation. A small discrepancy is noticed in the preceding trough before the focusing of the wave packet.
Further, the length of the numerical wave tank is reduced to 25 m and wave packets are generated with a focus distance $x_f = 15.0$ m and focus time $t_f = 15.0$ s. The numerical results are again compared with the results obtained from the 150 m long wave tank in Fig. (5). The focused wave height is slightly higher in the 25 m long wave tank compared to the 150 m long wave tank with an increase of 0.07 m in the focussed amplitude. The preceding trough is seen to be slightly shallower in the shorter 25 m long numerical wave tank compared to the longer 150 m long numerical wave tank. The results are considered to be satisfactory as the focussed amplitude is reproduced well in the shorter 25 m long domain compared to

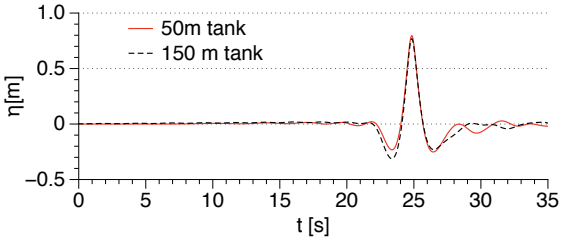


Figure 4: Wave gage at the focus point at $x_f = 35.0$ m for the 50 m tank compared to results from the 150 m tank with $x_f = 126.21$ m

the original 150 m long domain. The small discrepancy in the focussed amplitude follows from the fact that the wave packets in this shorter domain propagate over a much shorter distance and for a much shorter time before focussing. A grid convergence study is carried

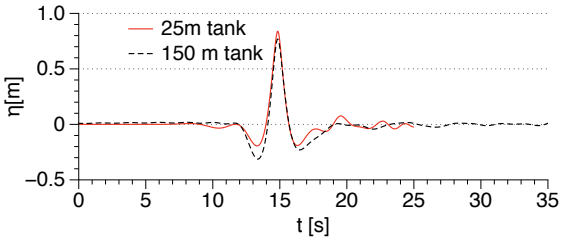


Figure 5: Wave gage at the focus point at $x_f = 15.0$ m for the 25 m tank compared to results from the 150 m tank with $x_f = 126.21$ m

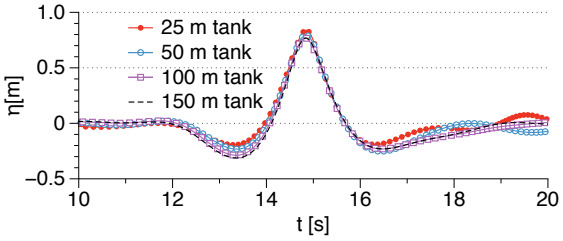


Figure 6: Comparison of free surface elevation at the focus point for all the different tank lengths simulated. The results are shifted along the $x-$axis to obtain a comparison of the focussed amplitude in the all the cases

out for the shorter numerical wave tank with a length of 25m, with focus point $x_f = 15.0$ m and $t_f = 15.0$ s with grid sizes $dx$= 0.1 m, 0.05 m, 0.075 m and 0.025 m. The comparison of the free surface elevations in the different simulations at the focus point is presented in Fig (7) and the numerical results at all the grid sizes are seen to be similar. The choice of the grid size of $dx = 0.05$ m is thus justified as it provides sufficiently accurate representation of the wave kinematics while being computationally efficient.

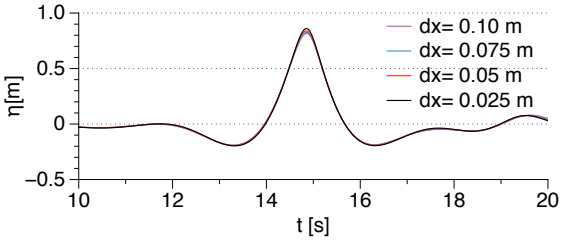


Figure 7: Comparison of free surface elevation at the focus point $x_f = 15.0$ m at time $t_f = 15.0$ s in a 25 m long numerical wave tank

## Focused wave breaking

In this part, the focus height of the wave packets is increased, so that breaking takes place. At first, the simulations are performed in an empty wave tank and a two-dimensional setup is sufficient for this case. Focused wave packets are generated in a 25 m long numerical wave tank with a water depth of $d = 4.01$ m with a focus amplitude of $A_f = 1.35$ m. The wave breaks at $x_b = 13.2$ m with a height of $H_b = 1.75$ m. Due to the non-linearities involved in waves of large amplitude and wave breaking, the propagating wave crest attains a vertical front earlier than the prescribed focus time of $t_f = 15.0$ s and at a location earlier than the focus distance of $x_f = 15.0$ m. The evolution of the breaking wave is shown in Figs. (8a-8e).

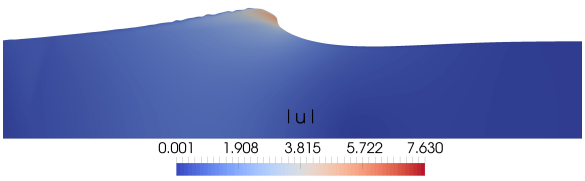


(a) $t = 13.55$ s

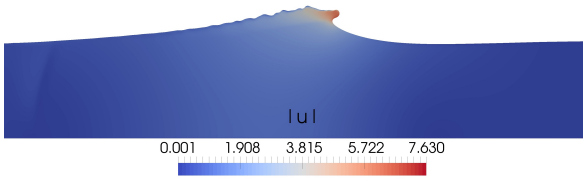


(b) $t = 14.00$ s

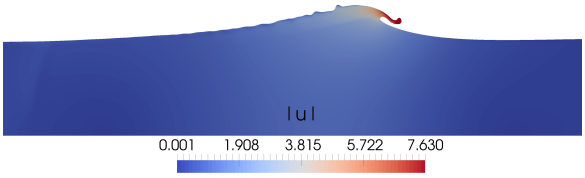


(c) $t = 14.40$ s

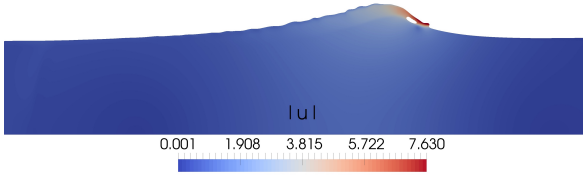


(d) $t = 14.60$ s

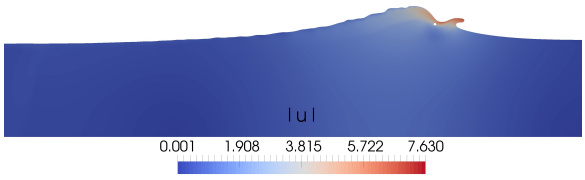


(e) $t = 14.85$ s

Figure 8: Evolution of the breaking wave produced by focussing wave packets with a target focus amplitude $A_f = 1.35$ m in a water depth of $d = 4.01$ m

## Breaking wave forces due to focussed wave breaking

The focused breaking wave packet presented in the previous section is simulated in a three-dimensional numerical wave tank of length 25 m and width 5 m with a water depth $d = 4.01$ m. A vertical cylinder with diameter $D = 0.7$ m is placed at $x = 15.0$ m. The wave breaking point is determined to be $x_b = 13.2$ m and the overturning wave crest impacts the surface of the cylinder just below the wave crest level at $x = 14.65$ m. This location of the cylinder with respect to the wave breaking point results in large breaking wave forces Irschik et al. (2002) Kamath et al. (under review). The calculated wave forces on the cylinder are presented in Fig. (9). The impulsive nature of breaking wave forces is seen in Fig.(9) with a sharp peak in the plot for wave force over time. The peak force occurs just after $t = 14.1$ s with a peak force of 17150 N. The evolution of the breaking wave and its interaction with the cylinder is presented in Figs. (10a-10e). The breaking wave with a vertical wave crest at 13.6 s is seen in Fig. (10a). Fig. (10b) shows the overturning wave crest approaching the front surface of the cylinder at $t = 13.8$ s, which impacts the cylinder at $t = 14.1$ s in Fig. (10c). The broken wave separating around the cylinder after impact is shown in Fig. (10d) and finally the formation of the water jet behind the cylinder formed after the interaction of the overturning wave crest with the cylinder is seen in Fig. (10e).

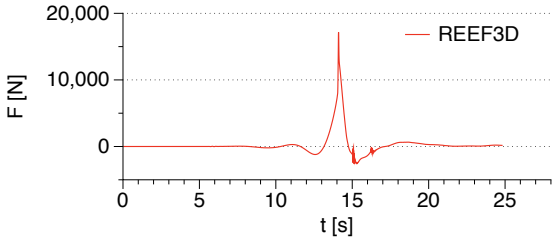


Figure 9: Breaking wave force on a vertical cylinder due focussed wave of amplitude $A_f = 1.35$ m

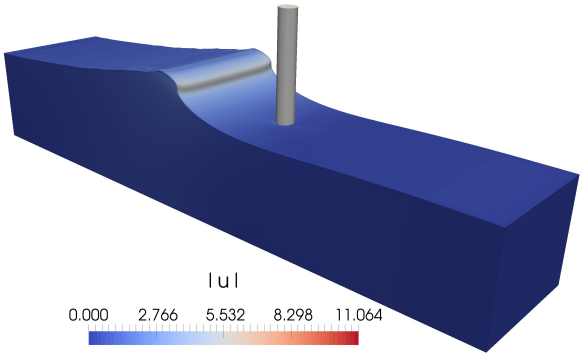


(a) $t = 13.6$ s

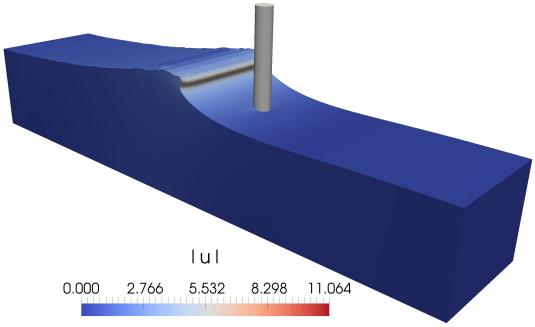


(b) $t = 13.8$ s

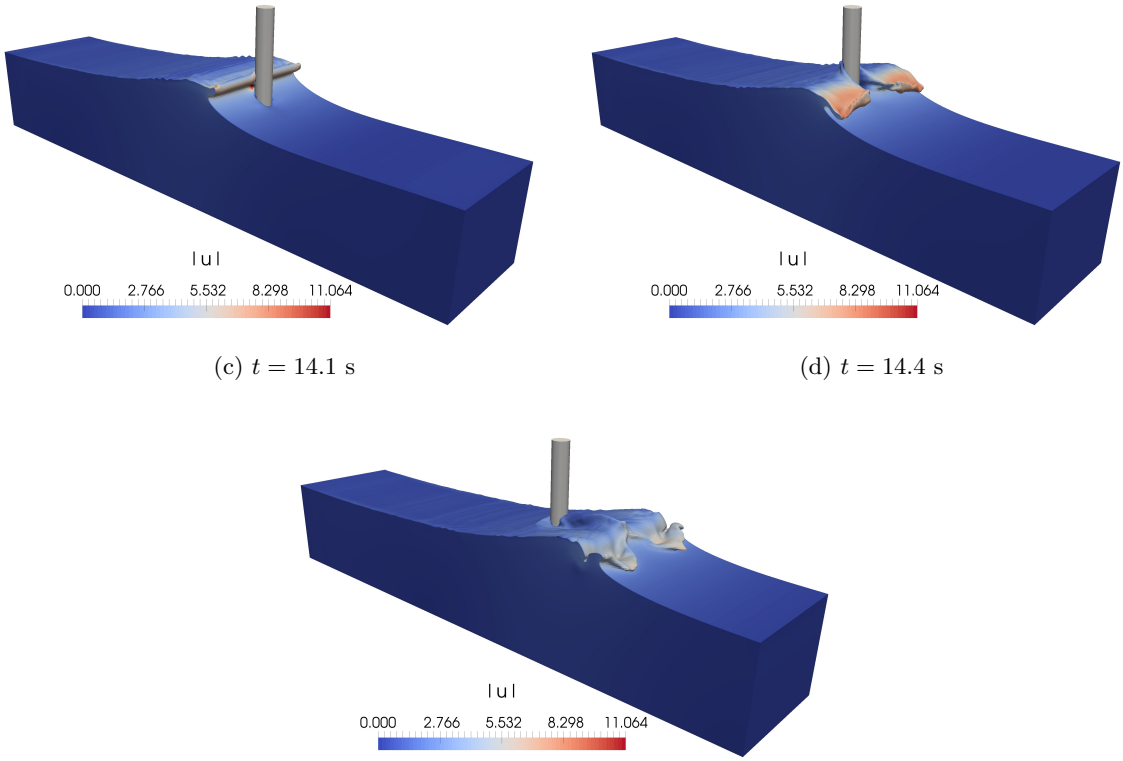


(c) $t = 14.1$ s

(d) $t = 14.4$ s

(e) $t = 14.9$ s

Figure 10: Interaction of the overturning wave crest with a vertical cylinder

# CONCLUSIONS

The open-source CFD model REEF3D is used in this study to generate focussed waves using wave packets. The implementation of the wave packets is validated by comparing the the numerical results with experimental results from the Large Wave Flume (GWK), Hannover, Germany. The numerical results showed a very good agreement with the experimental data, both for the generation and propagation of the wave packets in the numerical wave tank and for the replication of the focussed wave. Further simulations are carried out to replicate the focussed wave after propagation of the wave packets over a shorter distance and for a shorter time compared to the validation case. The numerical results for wave packet focussing after propagation over 15.0 m are found to be satisfactorily agree with the results from focussing after propagation over 126.21 m.

Further, simulations are carried out to induce deep water wave breaking using focussed wave packets. The breaking point and the breaker height are determined in two dimensional simulations. A three-dimensional simulation is then carried out to determine the breaking wave forces on a vertical cylinder. The breaking wave force due to a focused breaking wave with a breaker height of $H_b = 1.75$ m on a cylinder placed at a distance of $2D$ from the breaking point is calculated to be 17100 N. The interaction of the overturning wave crest with the cylinder is presented in detail.

## ACKNOWLEDGEMENTS

This research was supported in part with computational resources at NTNU provided by The Norwegian Metacenter for Computational Sciences (NOTUR, http://www.notur.no) under project no. NN2620K.

## References

Afzal, M.S., Bihs, H., Kamath, A. and Arntsen, Ø.A. (2015). Three-dimensional numerical modeling of pier scour under current and waves using level-set method. *Journal of Offshore Mechanics and Arctic Engineering*, **137**(3).

Alagan Chella, M., Bihs, H. and Muskulus, M. (2017). Solitary wave breaking and breaking wave forces on a vertically mounted circular cylinder over a sloping seabed. *Journal of Ocean Engineering and Marine Energy*, **3**(1), 1–19.

Alagan Chella, M., Bihs, H., Myrhaug, D. and Muskulus, M. (2016). Hydrodynamic characteristics and geometric properties of plunging and spilling breakers over impermeable slopes. *Ocean Modeling*, **103**, 53–72.

Ashby, S.F. and Flagout, R.D. (1996). A parallel mulitgrid preconditioned conjugate gradient algorithm for groundwater flow simulations. *Nuclear Science and Engineering*, **124**(1), 145–159.

Berthelsen, P.A. and Faltinsen, O.M. (2008). A local directional ghost cell approach for incompressible viscous flow problems with irregular boundaries. *Journal of Computational Physics*, **227**, 4354–4397.

Bihs, H., Alagan Chella, M., Kamath, A. and Arntsen, Ø.A. (2016*a*). Wave-structure interaction of focused waves with REEF3D. *OMAE 2016, 35th International Conference on Ocean, Offshore Arctic Engineering, Busan, South Korea*.

Bihs, H. and Kamath, A. (2016). Simulation of floating bodies with a combined level set/ghost cell immersed boundary representation. *International Journal for Numerical Methods in Fluids*.

Bihs, H., Kamath, A., Alagan Chella, M., Aggarwal, A. and Arntsen, Ø.A. (2016*b*). A new level set numerical wave tank with improved density interpolation for complex wave hydrodynamics. *Computers & Fluids*. 10.1115/OMAE2017-6152410.1016/j.compfluid.2016.09.012.

Center for Applied Scientific Computing, L.L.N.L. (2015). *HYPRE high performance preconditioners - User's Manual*.

Chen, L.F., Zang, J., Hillis, A.J., Morgan, G.C.J. and Plummer, A.R. (2014). Numerical investigation of wave–structure interaction using openFOAM. *Ocean Engineering*, **88**, 91—109.

Chorin, A. (1968). Numerical solution of the Navier-Stokes equations. *Mathematics of Computation*, **22**, 745–762.

Clauss, G.F. and Bergmann, J. (1986). Gaussian wave packets -a new approach to seakeeping tests of ocean structures. *Applied Ocean Research*, **8**(4), 190 – 206.

Clauss, G.F. and Kuehnlein, W.L. (1997). A new tool for seakeeping test - nonlinear transient wave packets. *8th International Conference on the Behaviour of Off-Shore Structures, Delft, The Netherlands*.

Durbin, P.A. (2009). Limiters and wall treatments in applied turbulence modeling. *Fluid Dynamics Research*, **41**, 1–18.

Grotle, E.L., Bihs, H., Æsøy, V. and Pedersen, E. (2016). CFD simulations of non-linear sloshing in a rotating rectangular tank with the level set method. *OMAE 2016, 35th International Conference on Ocean, Offshore Arctic Engineering, Busan, South Korea*.

Harten, A. (1983). High resolution schemes for hyperbolic conservation laws. *Journal of Computational Physics*, **49**, 357–393.

Henning, J. (2005). *Generation and Analysis of Harsh Wave Environments*. Ph.D. thesis, Technical University Berlin.

Irschik, K., Sparboom, U. and Oumeraci, H. (2002). Breaking wave characteristics for the loading of a slender pile. In: *Proc. 28th International Conference on Coastal Engineering, Cardiff, Wales*.

Jiang, G.S. and Shu, C.W. (1996). Efficient implementation of weighted ENO schemes. *Journal of Computational Physics*, **126**, 202–228.

Kamath, A., Alagan Chella, M., Bihs, H. and Arntsen, Ø.A. (under review). Breaking wave interaction with a vertical cylinder and the effect of breaker location. *Ocean Engineering*.

Naot, D. and Rodi, W. (1982). Calculation of secondary currents in channel flow. *Journal of the Hydraulic Division, ASCE*, **108**(8), 948–968.

Ning, D.Z., Zang, J., Liu, S.X., Eatock Taylor, R., Teng, B. and Taylor, P.H. (2009). Free-surface evolution and wave kinematics for nonlinear uni-directional focused wave groups. *Ocean Engineering*, **36**, 1226—1243.

Pakozdi, C. (2005). Numerische Simulation nichtlinearer transienter Wellengruppen. Report, Technical University Berlin.

Paulsen, B.T., Bredmose, H. and Bingham, H.B. (2014). An efficient domain decomposition strategy for wave loads on surface piercing circular cylinders. *Coastal Engineering*, **86**, 57–76.

Schäffer, H.A. (1996). Second-order wavemaker theory for irregular waves. *Ocean Engineering*, **23**(1), 47–88.

Sussman, M., Smereka, P. and Osher, S. (1994). A level set approach for computing solutions to incompressible two-phase flow. *Journal of Computational Physics*, **114**, 146–159.

Wienke, J. and Oumeraci, H. (2005). Breaking wave impact force on a vertical and inclined slender pile – theoretical and large-scale model investigations. *Coastal Engineering*, **52**, 435–462.

Wilcox, D.C. (1994). *Turbulence modeling for CFD.* DCW Industries Inc., La Canada, California.